Los Alamos
NATIONAL LABORATORY
memorandum

Los Alamos Neutron Science Center, LANSCE-1
Accelerator Physics and Engineering Group

To: Distribution
From: Barbara Blind, LANSCE-1, H808
Robert Garnett, LANSCE-1, H817
Phone/Fax: 5-2607/5-2904
Symbol: LANSCE-1:99-061
Date: April 5, 1999
Email: bblind@lanl.gov

SUBJECT: SNS Baseline MEBT and Modified Baseline MEBT

Introduction

We briefly describe the 18-quadrupole baseline MEBT of the SNS accelerator complex, specified by John Staples at LBNL. We also describe a modified baseline MEBT with improved properties. We call it the modified baseline MEBT because it has the same geometry as the baseline MEBT and only the settings of some of the quadrupoles and bunchers were adjusted. We will report on a 14-quadrupole MEBT, also specified by John Staples, at a later date.

Particle-tracking studies were performed for the baseline MEBT and for the modified baseline MEBT, and the rms emittances and maximum beam extents through the machine from 2.5 MeV to 1 GeV were compared for the two cases.

The modified baseline MEBT restores the partially deflected beams to the axis downstream of the antichopper and has better separation between the undeflected and the fully deflected beam than the baseline MEBT. Additionally, the modified baseline MEBT produces less rms-emittance growth than the baseline MEBT.

The modified baseline MEBT thus presents an improvement over the baseline MEBT. However, even for the modified baseline MEBT, performance is unacceptable with the expected 5-mil error limits on the transverse alignment of the MEBT quadrupoles. Particle losses at the chopper and antichopper can be expected unless steering through the MEBT is provided or realignment of components is performed. Additionally, to assure that all fully deflected beam is stopped, some 0.1% to 0.2% of the undeflected beam must be removed by the chopper stopper.

Description of SNS MEBT

The SNS MEBT basically can be broken up into three sections: a section to match from the RFQ to the center section, a center section, and a section to match from the center section to the DTL.

The center section is the reason for the existence of the MEBT. It houses the chopper and antichopper needed to produce the beam time structure required by the storage ring; the

macropulse must be converted into 546-ns-long beam pulses with 295-ns-long gaps. The center section has the requirement that the beam must be deflected a sufficient amount and must have a sufficiently small size to where the chopper stopper will remove all of the fully deflected beam without, ideally, removing any of the undeflected beam. At the same time, the center section must be properly tuned to restore the partially deflected beam to the axis downstream of the antichopper.

The baseline MEBT (and thus the modified baseline MEBT), has six quadrupoles and one cavity in the first section, three quadrupole pairs and one cavity in the center section, and six quadrupoles and two cavities in the third section. Figure 1 shows a layout, generated by TRACE 3-D, of the MEBT and of the first two periods of the DTL. Figure 1 also shows the matched beam in the first period of the DTL, for the 2-MW (56-mA) machine.

Baseline MEBT

The components of the baseline MEBT, and their settings, are listed in Appendix A in PARMILA notation. The listing indicates the 18 quadrupoles (Q1 through Q18) and four buncher cavities (B1 through B4). It also indicates the approximate chopper-stopper location and the centers of the chopper and antichopper. The beam deflections caused by the chopper and antichopper are simulated by shifts in the y′ particle coordinates at the centers of the elements. To this end, a code modification was made that introduced a 20 card to PARMILA. Thus, for instance, the "trans1 18 20 0.0 0.0 0.0 0.02" card adds 0.02 rad (20 mrad) to the y′ coordinate of each particle at element 18, the center of the chopper.

We assessed the performance of the baseline MEBT, both with PARMILA and with TRACE 3-D.

Figure 2, top, shows the footprints of the undeflected and the fully deflected beam at the chopper-stopper location (assumed to be 4.0 cm downstream of quadrupole Q9), as calculated by PARMILA. The fully deflected beam is defined as a beam that has been deflected by the chopper by 20 mrad. The input beam for producing this plot, and all corresponding plots (Figure 2, bottom, and Figure 5, top and bottom), was a 9269-macroparticle output beam generated by PARMULT for the SNS RFQ with a particular set of random errors. The MEBT did not have errors for this PARMILA run, or the corresponding PARMILA runs. Clearly, the separation between the undeflected and the fully deflected beam is marginal.

The phase advance between the chopper and antichopper also was not set correctly, because the center section of the MEBT had been optimized with the cavity (B2) turned off. Thus, the fully deflected beam (with the aperture representing the chopper stopper pulled out so as to not stop the beam) did not return to the axis. Instead, its centroid executed betatron oscillations. In the MEBT downstream of the antichopper, the beam centroid was off axis by as much as 7 mm. This means that the centroids of partially deflected beams would have been off axis by corresponding amounts.

TRACE 3-D was used to understand the properties of the baseline MEBT. As an input beam, a beam with the parameters of the output beam of the SNS RFQ without errors was used. At the center of B2, this beam has Twiss parameters of α_x=0.116, β_x=0.312 m, α_y=–1.154, β_y=0.816 m.

Modified Baseline MEBT

The modified baseline MEBT was first adjusted to achieve the proper phase advance between chopper and antichopper. This entailed an adjustment of the settings of quadrupoles Q8 and Q11, from 25.410 T/m to 26.138 T/m.

Quadrupoles Q3, Q4, Q5 and Q6 were then used to achieve a beam with smaller vertical size and larger horizontal size at the chopper stopper, as compared to the beam of the baseline MEBT. More specifically, the quadrupoles were adjusted with TRACE 3-D to achieve a beam with α_x=0, β_x=1.2 m, α_y=0, β_y=0.5 m at the center of B2. This resulted in increased beam separation at the chopper stopper, and also in a somewhat larger beam footprint and reduced power density at the chopper stopper.

The match to the DTL was restored with quadrupoles Q15, Q16, Q17 and Q18 and buncher cavities B3 and B4. The listing of the modified baseline MEBT is given in Appendix B.

The 9269-macroparticle RFQ output beam was tracked through the modified baseline MEBT without errors to the approximate chopper-stopper location. Figure 2, bottom, shows the footprints of the undeflected and fully deflected beam at that location. There is noticeably better beam separation than for the baseline MEBT.

Rectangular apertures (7 cards) were used in the simulations for the modified baseline MEBT, to represent the aperture restrictions created by the chopper plates, and the edge of the chopper stopper. The PARMILA code was modified to include asymmetrically positioned rectangular apertures. The listing of Appendix B shows the use of these modified 7 cards. The line "trans1 30 7 2.0 0.37 –2.0 –2.0" indicates that element 30 is a rectangular aperture with x_{max}=2.0 cm, y_{max}=0.37 cm, x_{min}=–2.0 cm, y_{min}=–2.0 cm. For a 7 card with only two entries, x_{min}=–x_{max} and y_{min}=–y_{max}. Thus, the "trans1 17 7 2.0 0.75" card describes a rectangular aperture with x_{max}=2.0 cm, y_{max}=0.75 cm, x_{min}=–2.0 cm, y_{min}=–0.75 cm. With this modification, the new 7 card remains compatible with input decks that previously ran with the old 7 card. With the aperture describing the chopper stopper opened up, none of the 9269 macroparticles was lost at any of the remaining apertures.

Appendix B shows the optimized quadrupole and cavity settings. An iterative procedure was used to optimize the match to the DTL. The beam rms emittances and Twiss parameters determined by PARMILA in the MEBT were used as input to TRACE 3-D to determine the DTL matched input beam and then the MEBT matching-section (Q15 through Q18, B3 and B4) settings required to achieve the match. A beam was then transported through the DTL to verify the quality of the match. Figure 3 shows the beam-

profile plots from 2.5 MeV to 20 MeV in the MEBT and DTL. Figure 4 shows the beam phase-space plots at the end of the MEBT (top) and at the end of the DTL (bottom). For Figures 3 and 4, the input beam was an output beam of an RFQ without errors.

Other Modified Baseline MEBTs (Later Rejected)

It is possible to reduce the vertical beam size at the chopper stopper further, but two things happen. For one, there is increased halo formation. Also, there is loss of beam at the upstream end of the chopper and downstream end of the antichopper. These are the locations where β_y increases with decreasing β_y at the center of B2.

In a first example, we focused to α_x=0.0, β_x=1.2 m, α_y=0.0, β_y=0.4 m at the center of B2. The footprints of the undeflected and fully deflected beam at the chopper-stopper location are shown in Figure 5, top. For the undeflected beam, one macroparticle was lost at the downstream end of the antichopper. This was without errors in the MEBT.

In a second example, we focused to α_x=0.0, β_x=1.2 m, α_y=0.0, β_y=0.3 m at the center of B2. The footprints of the undeflected and fully deflected beam at the chopper-stopper location are shown in Figure 5, bottom. For the undeflected beam, two macroparticles were lost at the upstream end of the chopper and 11 at the downstream end of the antichopper. This was again without errors in the MEBT.

Figure 5 compared to Figure 2, bottom, shows an increased distance between the cores of the beams but approximately the same amount of halo between the beams. The amount of undeflected beam that needs to be removed to completely stop the deflected beam is actually larger for the β_y=0.3 m case than for the β_y=0.5 m case.

Due to the particle losses at the chopper and antichopper for β_y=0.4 m and β_y=0.3 m, we ruled out these cases.

Machine Performance with Baseline MEBT and Modified Baseline MEBT

We had already done a study of the machine performance with the baseline MEBT. This study had focused on the rms emittances through the machine and on the particle losses. The maximum beam extents in the machine had also been looked at. Recently, we did a similar study of machine performance for the machine with the modified baseline MEBT.

In both cases, we used the same ten output beams from RFQs with errors. Each output beam was generated by tracking the 10000-macroparticle RFQ input beam through an RFQ with a vane voltage that was between 100% and 110% of nominal and with a slope in the vane voltage of up to 2.5% (below average at the entrance and above average at the exit, or vice versa). The ten RFQ output beams had 9269, 9442, 9354, 9395, 9415, 9536, 9498, 9394, 9288, and 9408 macroparticles, respectively.

We paired each RFQ output beam with a MEBT, DTL and CCDTL/CCL with errors described by a particular set of random numbers. In one case, we had assumed the baseline MEBT, in the other case we assumed the modified baseline MEBT. The error limits used for the components of the MEBT and DTL are given in Table 1 and the error limits used for the components of the CCDTL and CCL are given in Table 2. In Table 2, a segment is defined as the accelerating structure between quadrupoles.

Table 1. Error limits for components of SNS MEBT and DTL.

description of error	limit on error
quadrupole transverse displacement	5.0 mil (a) / 2.0 mil (b)
quadrupole tilt	0.29°
quadrupole roll	0.25°
quadrupole-gradient error	0.25% (c) / 0.5% (d)
rf-field phase error in tank (not bunchers)	0.5°
rf-field amplitude error in tank (not bunchers)	0.5%
rf-field tilt error in tank	0.1%

(a) for baseline MEBT and DTL, (b) for modified baseline MEBT,
(c) for baseline MEBT and modified baseline MEBT, (d) for DTL

Table 2. Error limits for components of SNS CCDTL and CCL.

name of parameter	description of error	limit on error
EQD	quadrupole transverse displacement	0.0127 cm (5.0 mil)
EQT	quadrupole tilt	5.0 mrad
EQR	quadrupole roll	5.0 mrad
EQS	quadrupole-gradient error	0.25%
EDBC	error in distance between end gaps of adjacent segments	0.0127 cm (5.0 mil)
ECAVL	error in distance between adjacent gaps of a segment	0.00508 cm (2.0 mil)
ESD	segment transverse displacement	0.025 cm, at ends (a)
EFM	module field-amplitude error (dynamic)	0.25%
EPHM	module phase error (dynamic)	0.25°
EFSET	module field-amplitude error (static)	1.0%
EPSET	module phase error (static)	1.0°
EFS	segment field-amplitude error (static)	1.0%
EPHS	segment phase error (static)	0.0
EFTILT	field-amplitude tilt in module	1.0%, at ends (b)

(a) independent misalignments of the two ends, resulting in displacements and tilts
(b) low at one end and high at other end, or vice versa

For an error limit of e_l, the errors are randomly chosen between $-e_l$ and e_l.

For the baseline MEBT, there had been no 7 cards in the PARMILA deck describing the MEBT (see Appendix A). The study of the modified baseline MEBT was performed with essentially the elements of Appendix B. However, in both cases, the beam was artificially brought back to the axis prior to entering the DTL (an earlier decision to simulate steering in the MEBT in this fashion). This was done with the new 19 card (not shown in Appendix A or Appendix B).

For the study of the baseline MEBT, the limits for the transverse random misalignments of the MEBT quadrupoles had been at 5.0 mil, for the study of the modified baseline MEBT, they were at 2.0 mil. Since for the corresponding runs the random numbers were the same, a quadrupole of the baseline MEBT with a 5.0-mil misalignment corresponded to a quadrupole of the modified baseline MEBT with a 2.0-mil misalignment. We really should have taken out the apertures for this set of runs instead of trying to transport the beam with fewer losses by reducing the steering due to the quadrupole misalignments. Fortunately, misalignments will mainly contribute to steering and very little to emittance growth. Since the beam was artificially brought back on axis at the end of the MEBT, the beam centroid was further from the axis for the baseline MEBT, as compared to the modified baseline MEBT, through only a very few elements of the MEBT.

The gradient errors in the MEBT for corresponding cases were the same in the sense that the fractional gradient errors were the same. Thus, if Q8 of the baseline MEBT was 0.25% lower than its nominal setting of 25.410 T/m, then Q8 of the modified baseline MEBT was 0.25% lower than its nominal setting of 26.138 T/m.

Of the ten runs for the baseline MEBT, in run 7 one macroparticle was lost in the third buncher cavity of the MEBT and one macroparticle was lost in element 28 of the DTL. In runs 4 and 8, one macroparticle each was lost in element 3 of the CCDTL. These were the only particle losses.

For the modified baseline MEBT, 15, 9, 9, 12, 8, 8, 67, 11, 25, and 9 macroparticles, respectively, were removed by the chopper stopper and there were no losses anywhere else.

One could suspect that the removal of a number of macroparticles could significantly change the rms emittances of the beam. Therefore, the run with 67 macroparticles removed (run 7) was repeated with the aperture representing the chopper stopper opened up. The horizontal, vertical, and longitudinal rms emittance at the exit of the CCL were 0.0312 π-cm-mrad, 0.0312 π-cm-mrad and 0.0497 π-cm-mrad, respectively, for the case with 67 macroparticles removed and 0.0311 π-cm-mrad, 0.0321 π-cm-mrad and 0.0502 π-cm-mrad, respectively, for the case with no macroparticles removed. Thus, the results are not significantly affected by the removal of macroparticles. For the case with no macroparticles removed by the chopper stopper, there was one macroparticle lost in the antichopper and one in the DTL, similar to run 7 with the baseline MEBT.

Figure 6 shows the transverse and longitudinal rms emittances of the beam in the MEBT (top) and the transverse maximum beam extents in the MEBT (bottom). Figure 7 shows the same for the DTL and Figure 8 shows the same for the CCDTL and CCL. Figures 6, 7, and 8 are for the baseline MEBT. Figures 9, 10, and 11 show the corresponding plots for the modified baseline MEBT. The transverse rms emittances are somewhat smaller and have somewhat less spread for the modified baseline MEBT as compared to the baseline MEBT. They range between 0.0272 π-cm-mrad and 0.0312 π-cm-mrad for the modified baseline MEBT and between 0.0288 π-cm-mrad and 0.0342 π-cm-mrad for the baseline MEBT. The longitudinal rms emittances are clearly improved for the modified baseline MEBT compared to the baseline MEBT. They range between 0.0497 π-cm-mrad and 0.0616 π-cm-mrad, compared to between 0.0576 π-cm-mrad and 0.0720 π-cm-mrad, a 14% improvement.

As mentioned, a certain amount of undeflected beam was removed by the chopper stopper. Tracking through the modified baseline MEBT alone had initially been performed with the 5.0-mil limit on the transverse misalignments of the MEBT quadrupoles. In nine of the runs, the fully deflected beam was completely stopped by the aperture representing the chopper stopper, in one run (run 5) 78 particles missed this aperture. In the latter case, the beam centroid at the chopper stopper was at 0.656 cm, to be compared to a nominal value of 0.870 cm. From the ten undeflected beams, 19, 34, 4, 10, 3, 5, 108, 8, 50, and 1 macroparticles, respectively, were removed by the aperture representing the chopper stopper. Additionally, some macroparticles were removed at the chopper (7 in run 5 and 1 in run 8) and at the antichopper (9 in run 3, 147 in run 5, 20 in run 6, 5 in run 7 and 10 in run 10).

Clearly, some steering is required through the chopper and antichopper, or else allowance has to be made for realignment of components. As mentioned before, when performing the computations under the assumption of a 2.0-mil limit on the transverse misalignments of the MEBT quadrupoles to simulate partial steering, there are no particle losses in the chopper or antichopper.

Finally, when tracking each of the ten RFQ output beams through the MEBT with the errors of run 1 (2.0-mil error limit on the transverse misalignments of the MEBT quadrupoles), the numbers of macroparticles removed by the aperture representing the chopper stopper are 15, 5, 19, 15, 23, 11, 16, 17, 11, and 17.

Table 3 sums up the numbers quoted above. Shown are the number of macroparticles in each input beam, followed by the number of macroparticles removed by the chopper stopper, chopper and antichopper, first for the 5.0-mil limit and then for the 2.0-mil limit on the transverse misalignment of the MEBT quadrupoles.

In order to assure that all of the fully deflected beam is removed by the chopper stopper, some 0.1% to 0.2% of the undeflected beam must be removed as well. This is evident from the computations, as well as from inspecting Figure 2, bottom.

Table 3. Number of macroparticles that (1) enter MEBT, (2 and 5) are removed by chopper stopper, (3 and 6) are removed by plates of chopper, (4 and 7) are removed by plates of antichopper. Columns 2, 3, 4 are for 5.0-mil limits and columns 5, 6, 7 are for 2.0-mil limits on transverse misalignments of MEBT quadrupoles. Column 8 shows number of macroparticles removed by chopper stopper for indicated input beam going through MEBT with errors of run 1. All numbers are for modified baseline MEBT and undeflected beam.

1	2	3	4	5	6	7	8
9269	19	0	0	15	0	0	15
9442	34	0	0	9	0	0	5
9354	4	0	9	9	0	0	19
9395	10	0	0	12	0	0	15
9415	3	7	147	8	0	0	23
9536	5	0	20	8	0	0	11
9498	108	0	5	67	0	0	16
9394	8	1	0	11	0	0	17
9288	50	0	0	25	0	0	11
9408	1	0	10	9	0	0	17

Appendix A. Excerpt from PARMILA input deck for baseline MEBT.

```
trans1 1  1   0.0e-1    1      2.0  0 1 1
trans1 2  1   3.5       2      2.0  0 1 1
trans1 3  3   2226.9  7.0       2.0  1 1 1              Q1
trans1 4  1   5.0       2      2.0  0 1 1
trans1 5  3  -2500.0  7.0       2.0  1 1 1              Q2
trans1 6  1   6.0       2      2.0  0 1 1
trans1 7  3   2400.0  7.0       2.0  1 1 1              Q3
trans1 8  1   6.0       2      2.0  0 1 1
trans1 9  3  -2575.6  7.0       2.0  1 1 1              Q4
trans1 10 1   6.0       3      2.0  0 1 1
trans1 11 3   2100.0  7.0       2.0  1 1 1              Q5
trans1 12 1  10.0       5      2.0  0 1 1
trans1 13 2  0.070    -90.     1  2.0 1 1              B1
trans1 14 1   8.0       4      2.0  0 1 1
trans1 15 3  -1070.0  7.0       2.0  1 1 1              Q6
trans1 16 1   3.5       2      2.0  0 1 1
-------------------------------------------------------------------------------------------------
trans1 17 1   25.0      10       2.0  0 1 1
trans1 18 20 0.0 0.0 0.0 0.02                          center of chopper
trans1 19 1   25.0      10       2.0  0 1 1
trans1 20 1   4.0       2      2.0  0 1 1
trans1 21 3  -1600.0  7.0       2.0  1 1 1              Q7
trans1 22 1   3.0       2      2.0  0 1 1
trans1 23 3   2541.0  7.0       2.0  1 1 1              Q8
trans1 24 1   3.0       2      2.0  0 1 1
trans1 25 3  -1100.0  7.0       2.0  1 1 1              Q9
trans1 26 1   4.0       4      2.0  0 1 1
                                                       approximate chopper stopper location
trans1 27 1   4.0       4      2.0  0 1 1
trans1 28 2  0.060    -90.     1  2.0 1 1              B2
trans1 29 1   8.0       4      2.0  0 1 1
trans1 30 3  -1100.0  7.0       2.0  1 1 1              Q10
trans1 31 1   3.0       2      2.0  0 1 1
trans1 32 3   2541.0  7.0       2.0  1 1 1              Q11
trans1 33 1   3.0       2      2.0  0 1 1
trans1 34 3  -1600.0  7.0       2.0  1 1 1              Q12
trans1 35 1   4.0       2      2.0  0 1 1
trans1 36 1   25.0      10       2.0  0 1 1
trans1 37 20 0.0 0.0 0.0 0.02                          center of anti chopper
trans1 38 1   25.0      10       2.0  0 1 1
-------------------------------------------------------------------------------------------------
trans1 39 1   3.5       2      2.0  0 1 1
trans1 40 3  -1000.0  7.0       2.0  1 1 1              Q13
trans1 41 1   6.0       3      2.0  0 1 1
trans1 42 2  0.04256     -90.    1  2.0 1 1                        B3
trans1 43 1   6.0       3      2.0  0 1 1
trans1 44 3   1900.0  7.0       2.0  1 1 1              Q14
trans1 45 1   6.0       3      2.0  0 1 1
trans1 46 3  -2292.96 7.0       2.0  1 1 1              Q15
trans1 47 1   6.0       3      2.0  0 1 1
trans1 48 3   2141.18 7.0       2.0  1 1 1              Q16
trans1 49 1   6.0       3      2.0  0 1 1
trans1 50 2  0.07766     -90.    1  2.0 1 1                        B4
trans1 51 1   6.0       3      2.0  0 1 1
trans1 52 3  -1565.56 7.0       2.0  1 1 1              Q17
trans1 53 1   5.0       2      2.0  0 1 1
trans1 54 3   638.05   7.0       2.0  1 1 1              Q18
trans1 55 1  17.0       3      2.0  0 1 1
trans1 56 3  -6700.0  1.75     1.25  0 1 1
```

Appendix B. Excerpt from PARMILA input deck for modified baseline MEBT.

```
trans1 1  1   0.0e-1    1      2.0  0 1 1
trans1 2  1   3.5       2      2.0  0 1 1
trans1 3  3   2226.9  7.0      2.0  1 1 1
trans1 4  1   5.0       2      2.0  0 1 1
trans1 5  3  -2500.0  7.0      2.0  1 1 1
trans1 6  1   6.0       2      2.0  0 1 1
trans1 7  3   2402.172  7.0      2.0  1 1 1
trans1 8  1   6.0       2      2.0  0 1 1
trans1 9  3  -2823.475  7.0      2.0  1 1 1
trans1 10 1   6.0       3      2.0  0 1 1
trans1 11 3   2132.818  7.0      2.0  1 1 1
trans1 12 1  10.0       5      2.0  0 1 1
trans1 13 2  0.070    -90.     1  2.0 1 1
trans1 14 1   8.0       4      2.0  0 1 1
trans1 15 3  -762.065  7.0      2.0  1 1 1
trans1 16 1   3.5       2      2.0  0 1 1
trans1 17 7  2.0 0.75
trans1 18 1   25.0     10      2.0  0 1 1
trans1 19 7  2.0 0.75
trans1 20 20 0.0 0.0 0.0 0.00
trans1 21 1   25.0     10      2.0  0 1 1
trans1 22 7  2.0 1.0 -2.0 -.5
trans1 23 1   4.0       2      2.0  0 1 1
trans1 24 3  -1600.0  7.0      2.0  1 1 1
trans1 25 1   3.0       2      2.0  0 1 1
trans1 26 3   2613.783  7.0      2.0  1 1 1
trans1 27 1   3.0       2      2.0  0 1 1
trans1 28 3  -1100.0  7.0      2.0  1 1 1
trans1 29 1   4.0       4      2.0  0 1 1
trans1 30 7  2.0  0.37  -2.0 -2.0
trans1 31 1   4.0       4      2.0  0 1 1
trans1 32 2  0.060    -90.     1  2.0 1 1
trans1 33 1   8.0       4      2.0  0 1 1
trans1 34 3  -1100.0  7.0      2.0  1 1 1
trans1 35 1   3.0       2      2.0  0 1 1
trans1 36 3   2613.783  7.0      2.0  1 1 1
trans1 37 1   3.0       2      2.0  0 1 1
trans1 38 3  -1600.0  7.0      2.0  1 1 1
trans1 39 1   4.0       2      2.0  0 1 1
trans1 40 7  2.0 1.0 -2.0 -0.5
trans1 41 1   25.0     10      2.0  0 1 1
trans1 42 7  2.0 0.75
trans1 43 20 0.0 0.0 0.0 0.00
trans1 44 1   25.0     10      2.0  0 1 1
trans1 45 7  2.0 0.75
trans1 46 1   3.5       2      2.0  0 1 1
trans1 47 3  -1000.0  7.0      2.0  1 1 1
trans1 48 1   6.0       3      2.0  0 1 1
trans1 49 2  0.030461     -90.    1  2.0 1 1
trans1 50 1   6.0       3      2.0  0 1 1
trans1 51 3   1900.0  7.0      2.0  1 1 1
trans1 52 1   6.0       3      2.0  0 1 1
trans1 53 3  -1854.43 7.0      2.0  1 1 1
trans1 54 1   6.0       3      2.0  0 1 1
trans1 55 3   1965.57 7.0      2.0  1 1 1
trans1 56 1   6.0       3      2.0  0 1 1
trans1 57 2  0.10595     -90.    1  2.0 1 1
trans1 58 1   6.0       3      2.0  0 1 1
trans1 59 3  -2310.56 7.0      2.0  1 1 1
trans1 60 1   5.0       2      2.0  0 1 1
trans1 61 3   1310.52   7.0     2.0  1 1 1
trans1 62 1  17.0       3      2.0  0 1 1
```

trans1 63 3 -6700.0 1.75 1.25 0 1 1

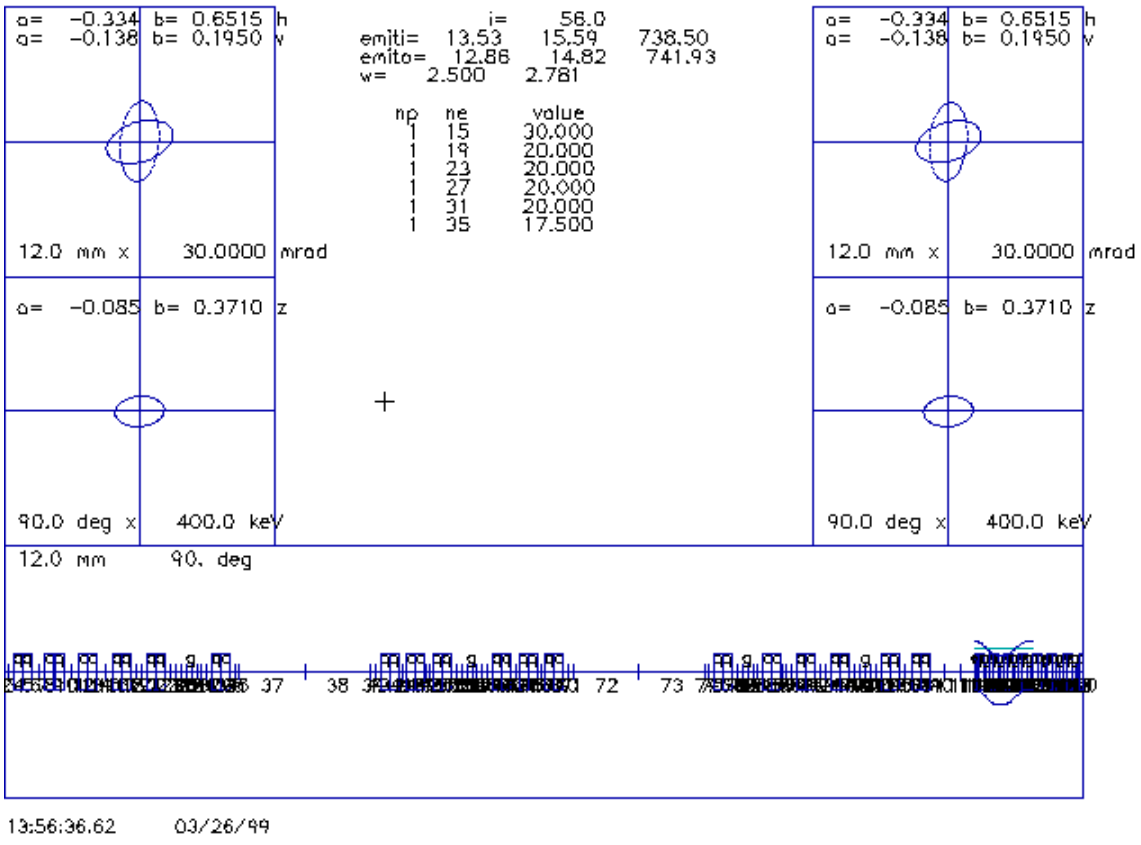

Figure 1. Layout of SNS baseline MEBT and first two periods of DTL.

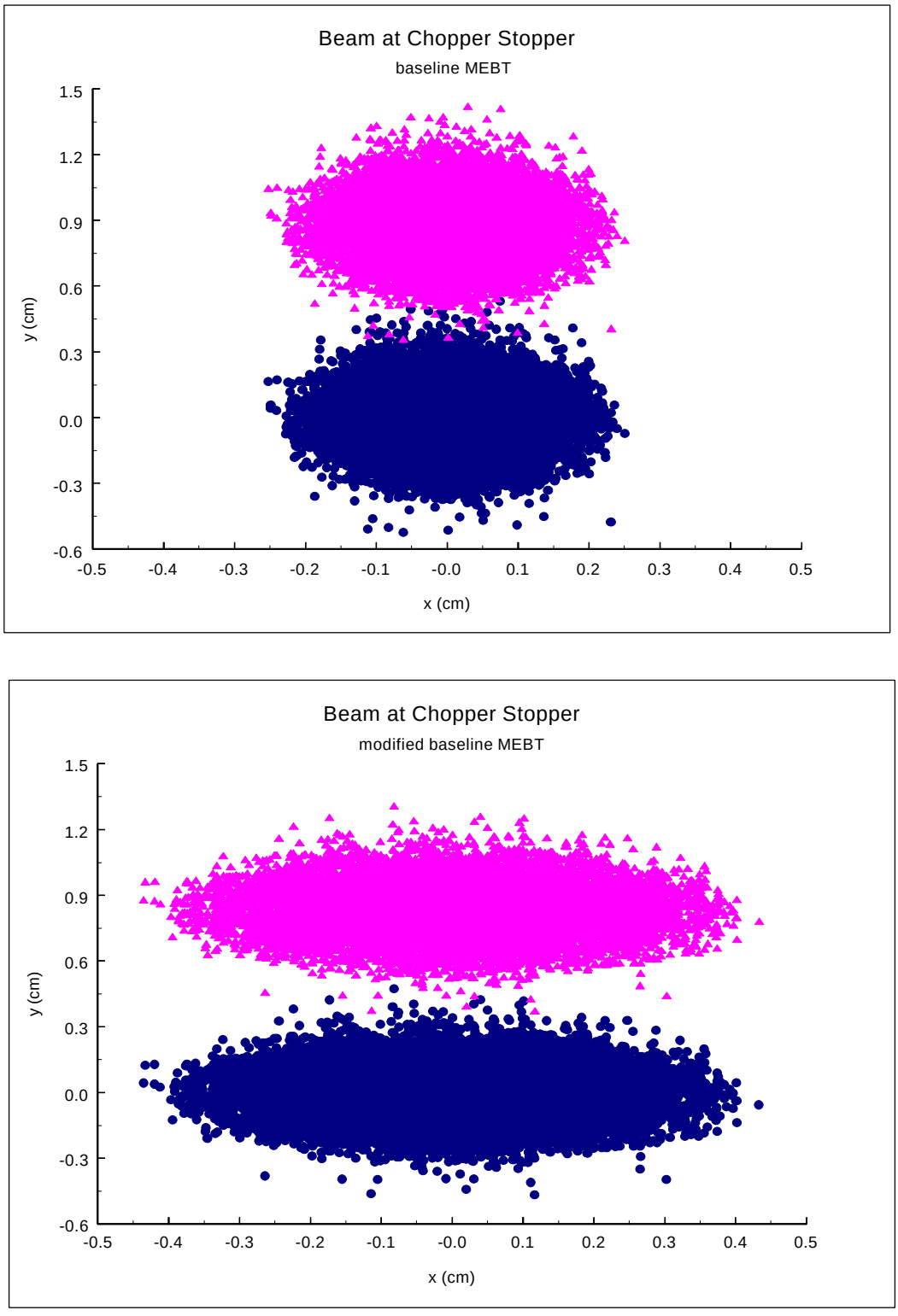

Figure 2. Undeflected and fully deflected beam at chopper stopper, for baseline MEBT (top) and modified baseline MEBT (bottom).

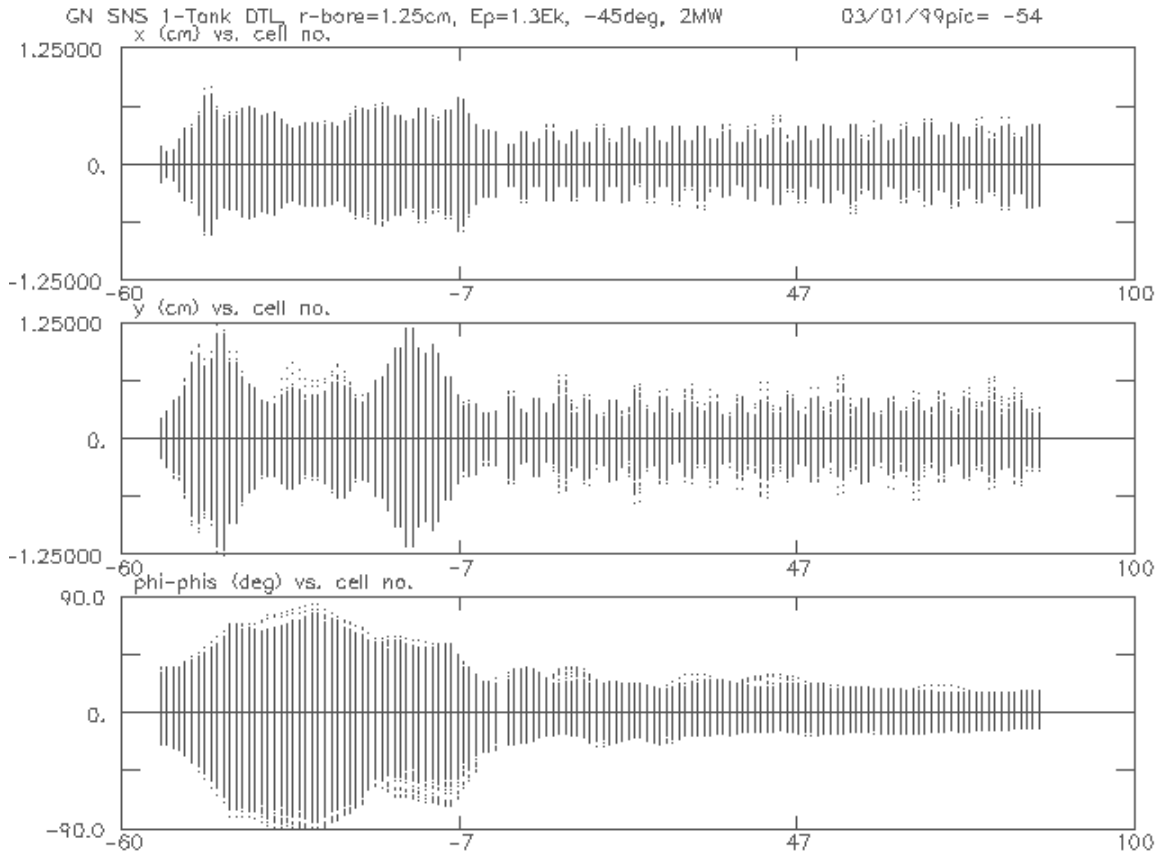

Figure 3. Beam-profile plots through MEBT and DTL, from 2.5 MeV to 20.0 MeV.

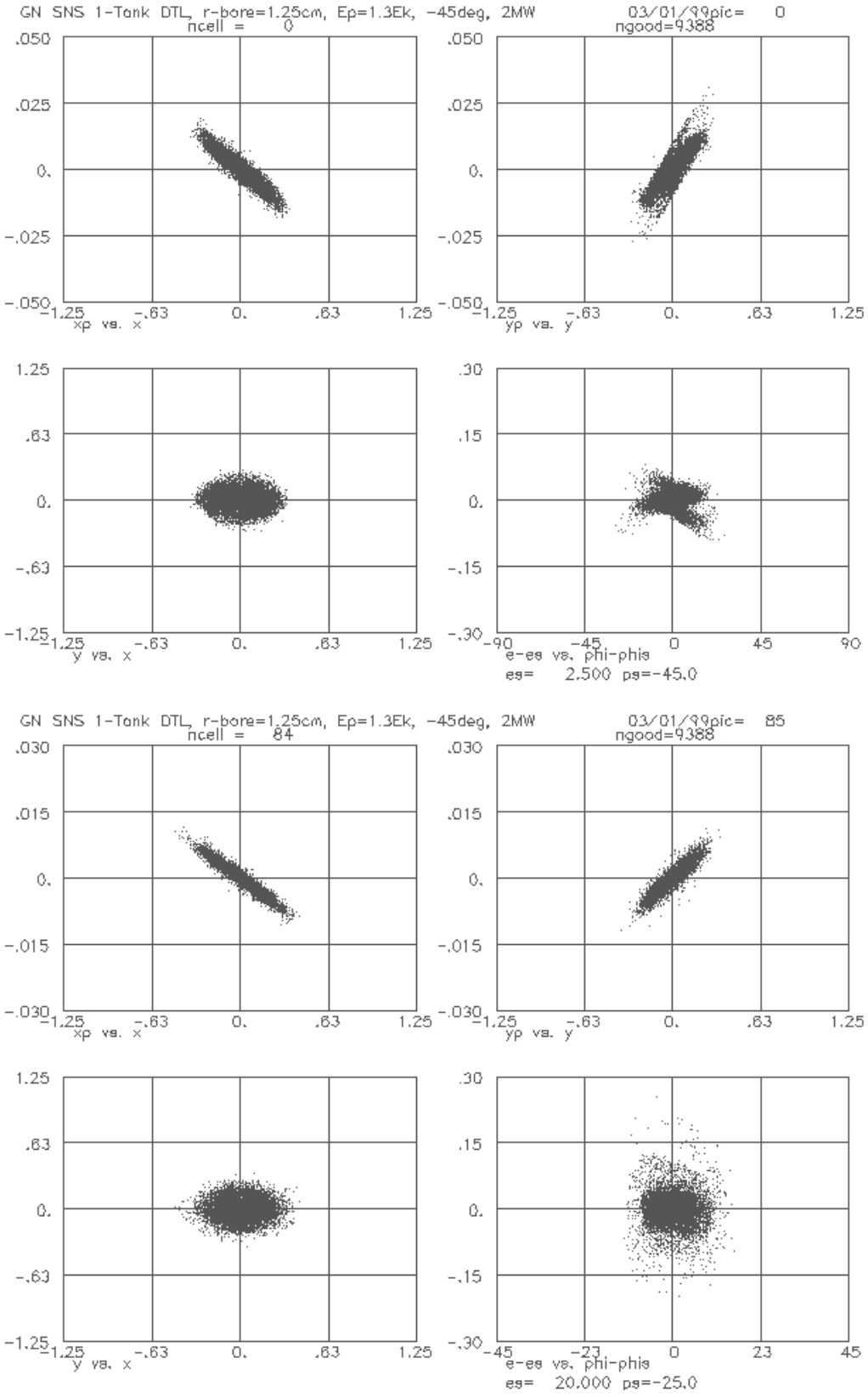

Figure 4. Beam phase-space plots at end of MEBT (top) and at end of DTL (bottom).

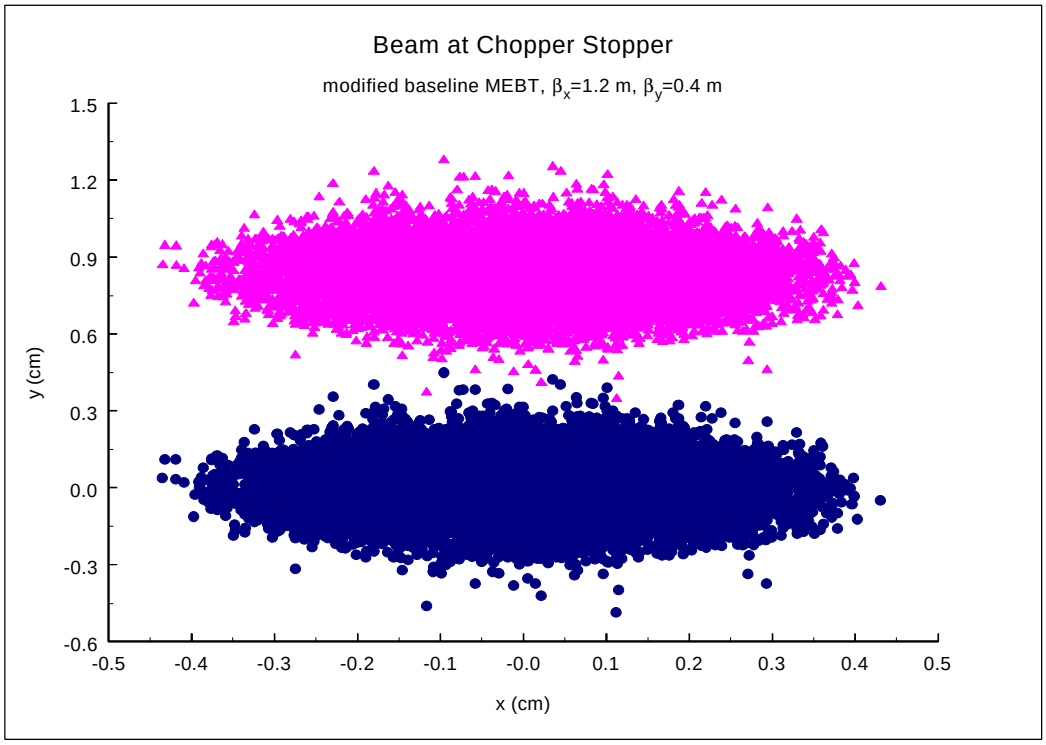

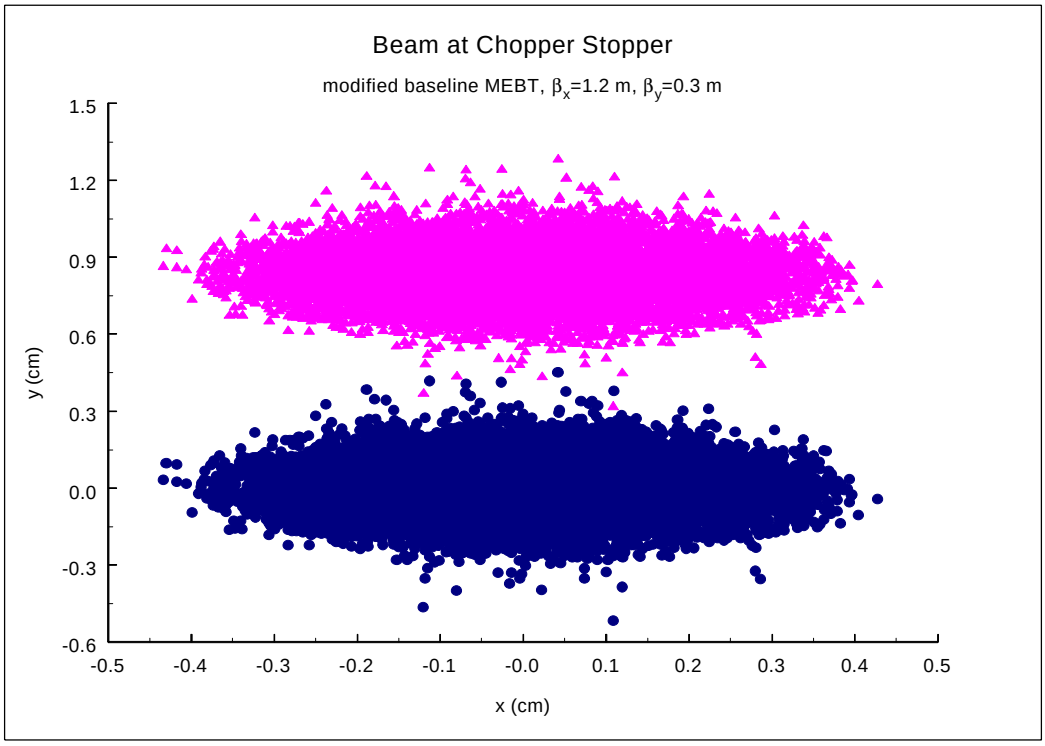

Figure 5. Undeflected and fully deflected beam at chopper stopper, for modified baseline MEBTs with β_x=1.2 m, β_y=0.4 m (top) and β_x=1.2 m, β_y =0.3 m (bottom).

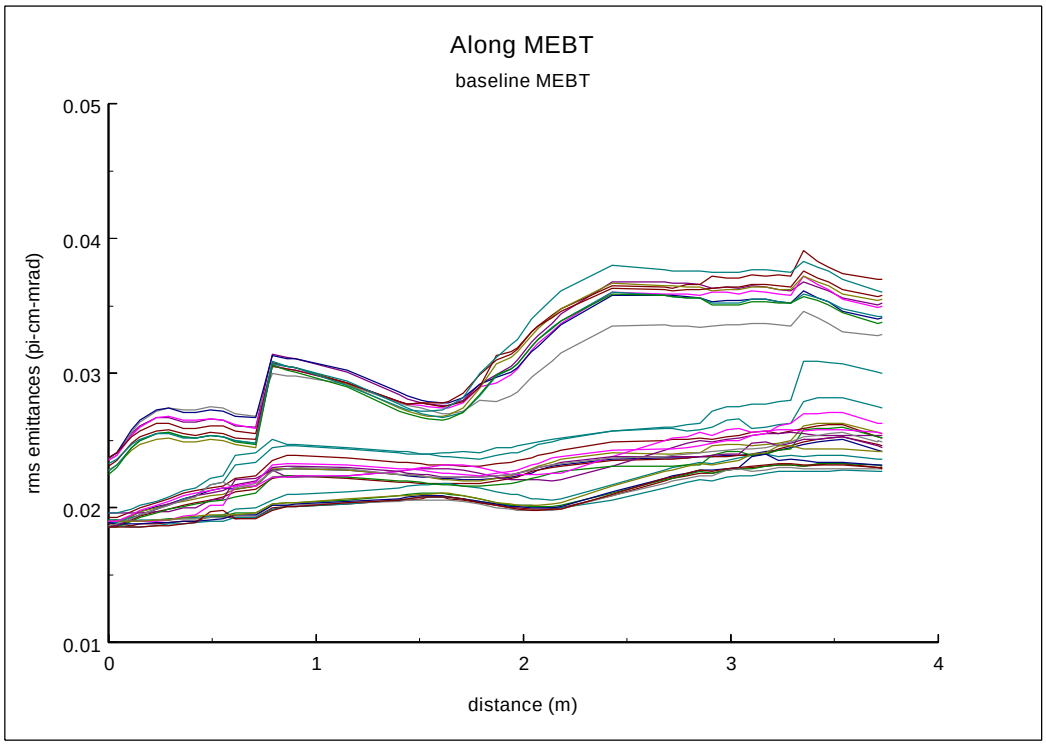

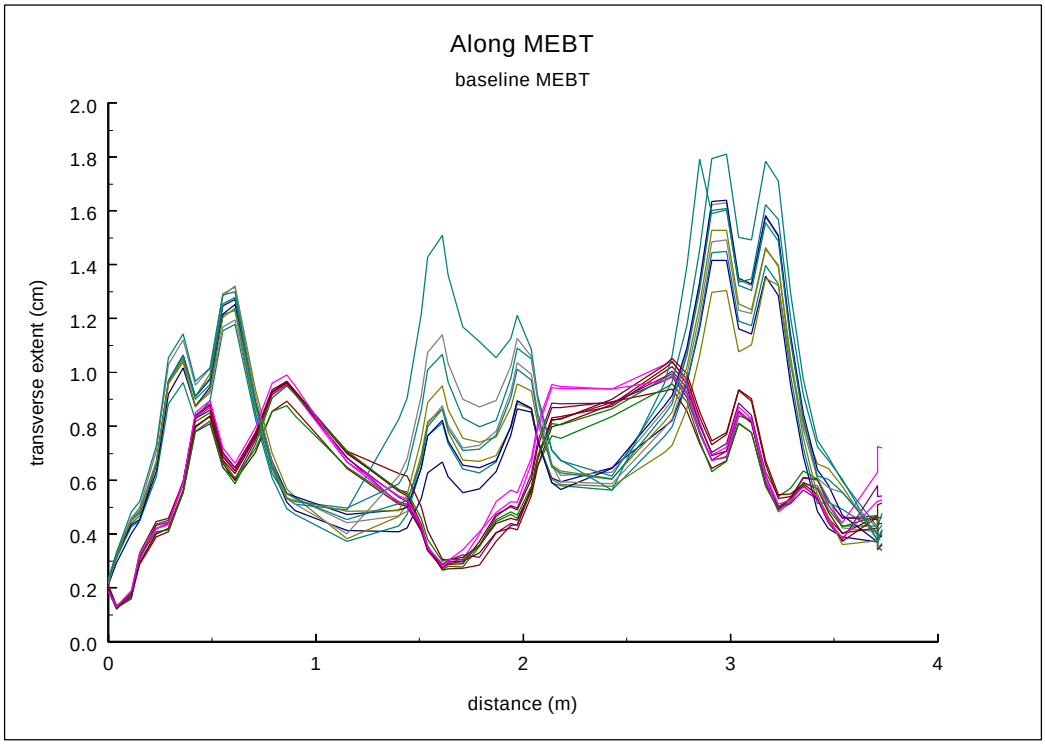

Figure 6. Transverse and longitudinal rms emittances (top) and transverse maximum beam extents (bottom) in MEBT, for baseline MEBT.

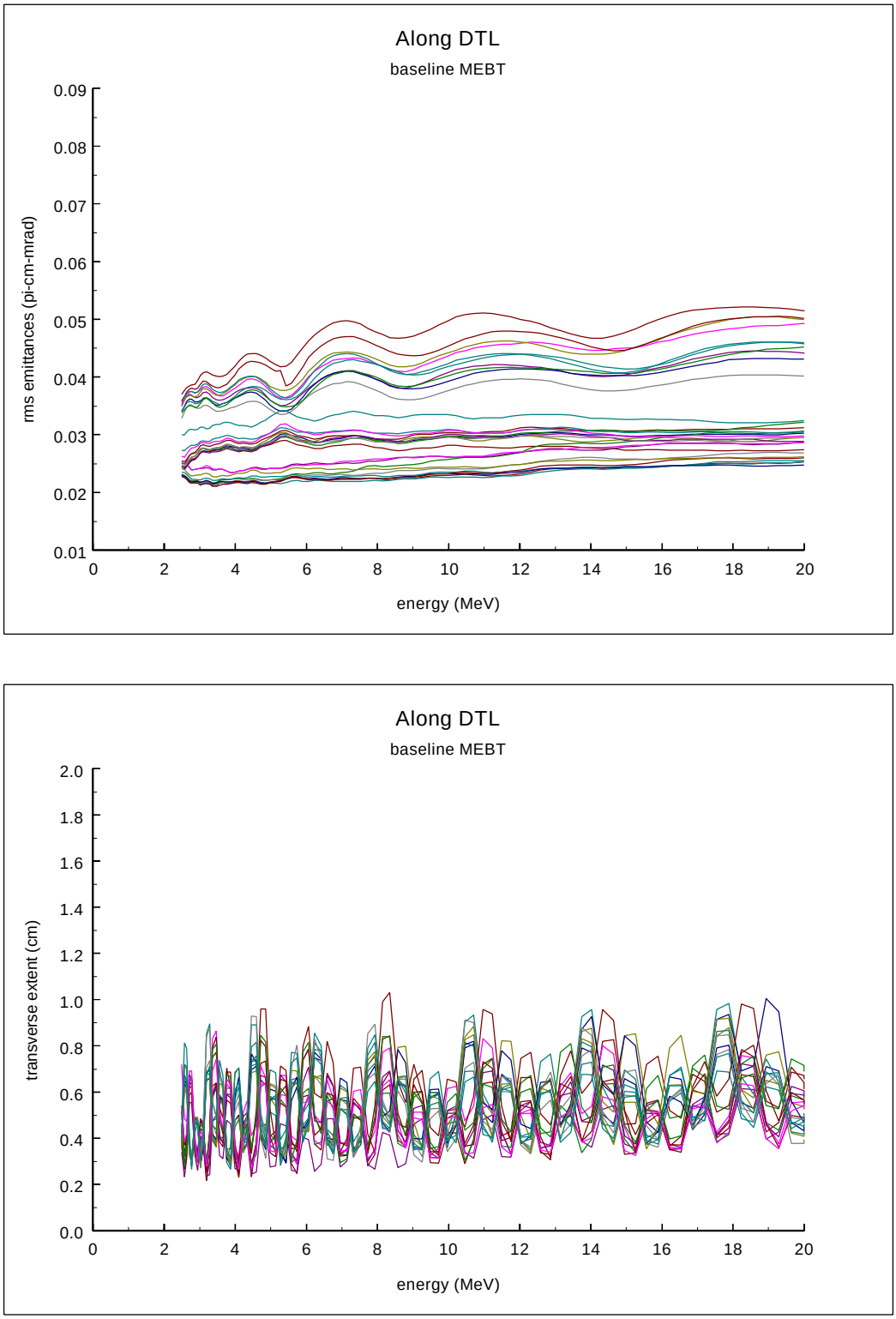

Figure 7. Transverse and longitudinal rms emittances (top) and transverse maximum beam extents (bottom) in DTL, for baseline MEBT.

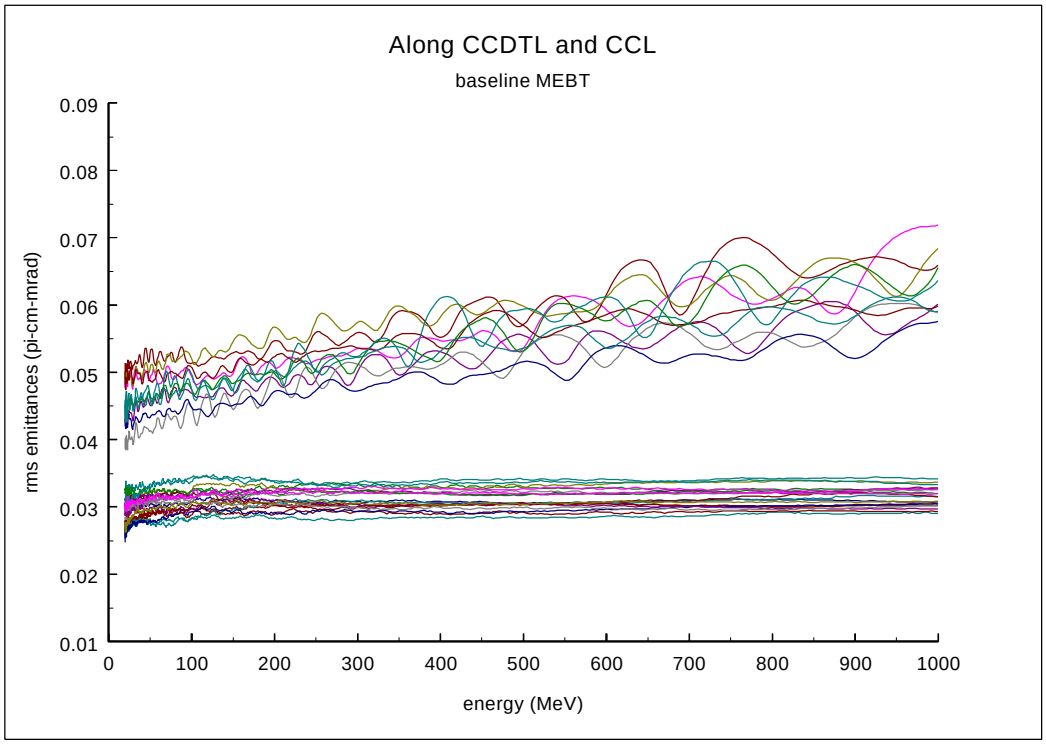

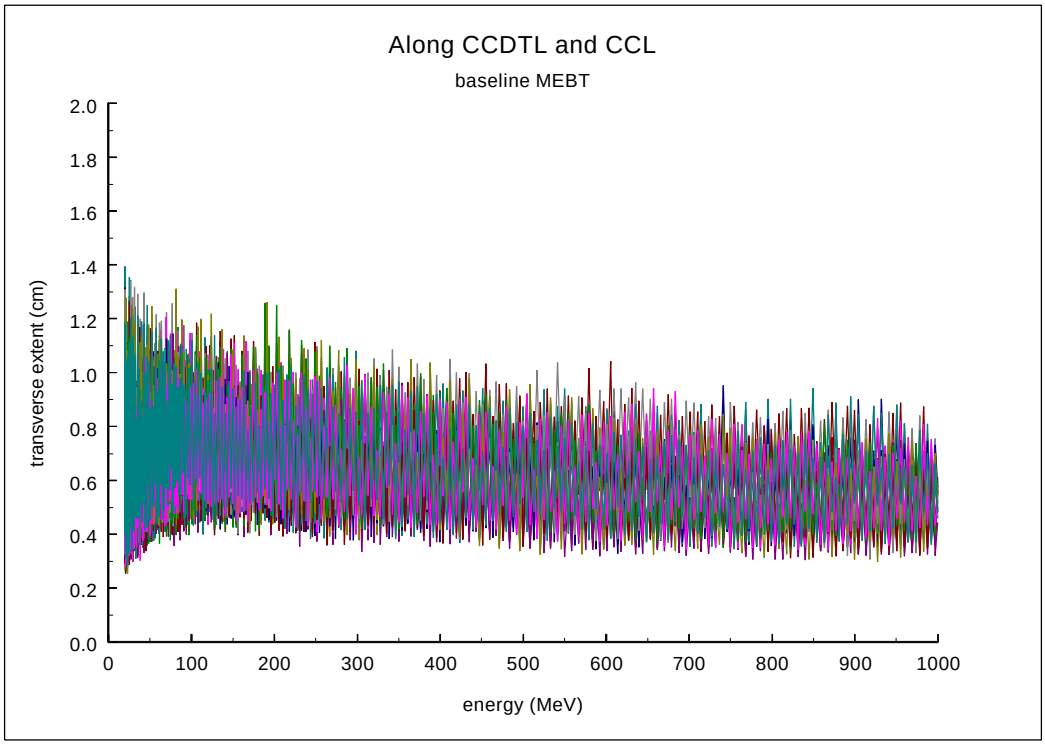

Figure 8. Transverse and longitudinal rms emittances (top) and transverse maximum beam extents (bottom) in CCDTL and CCL, for baseline MEBT.

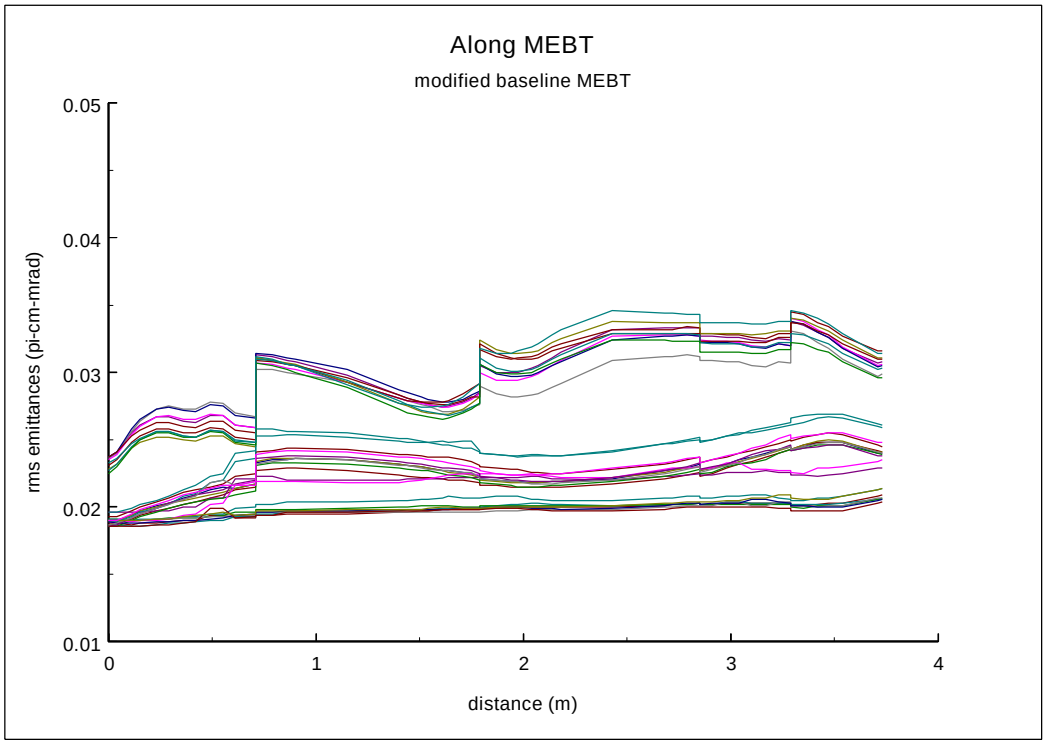

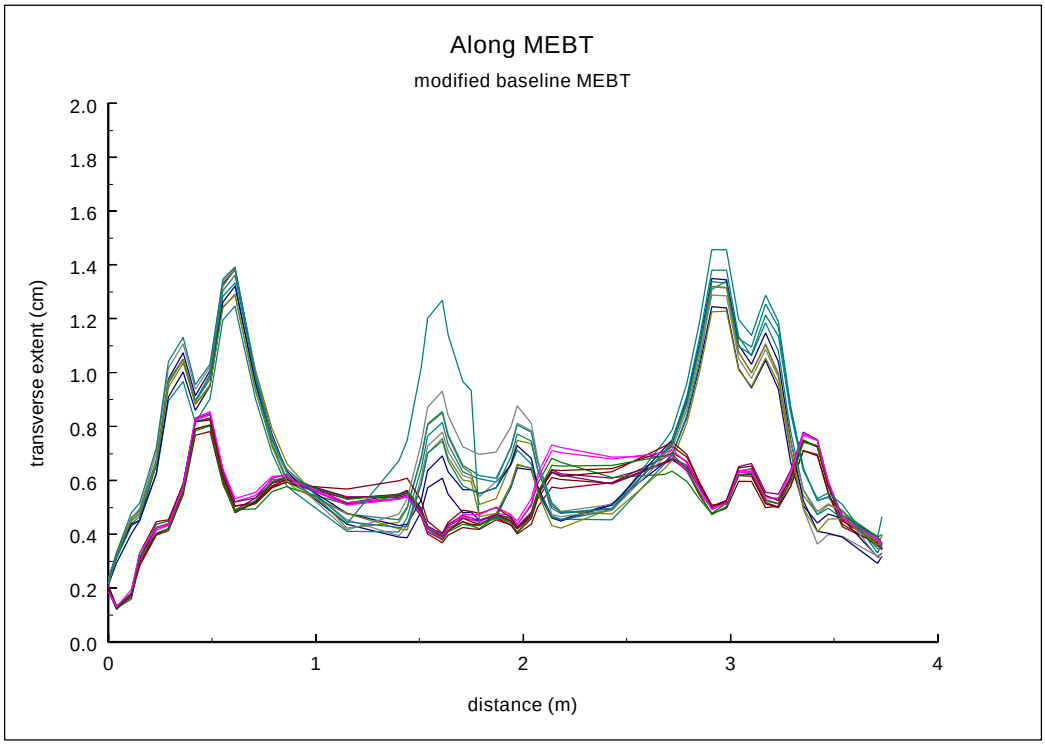

Figure 9. Transverse and longitudinal rms emittances (top) and transverse maximum beam extents (bottom) in MEBT, for modified baseline MEBT.

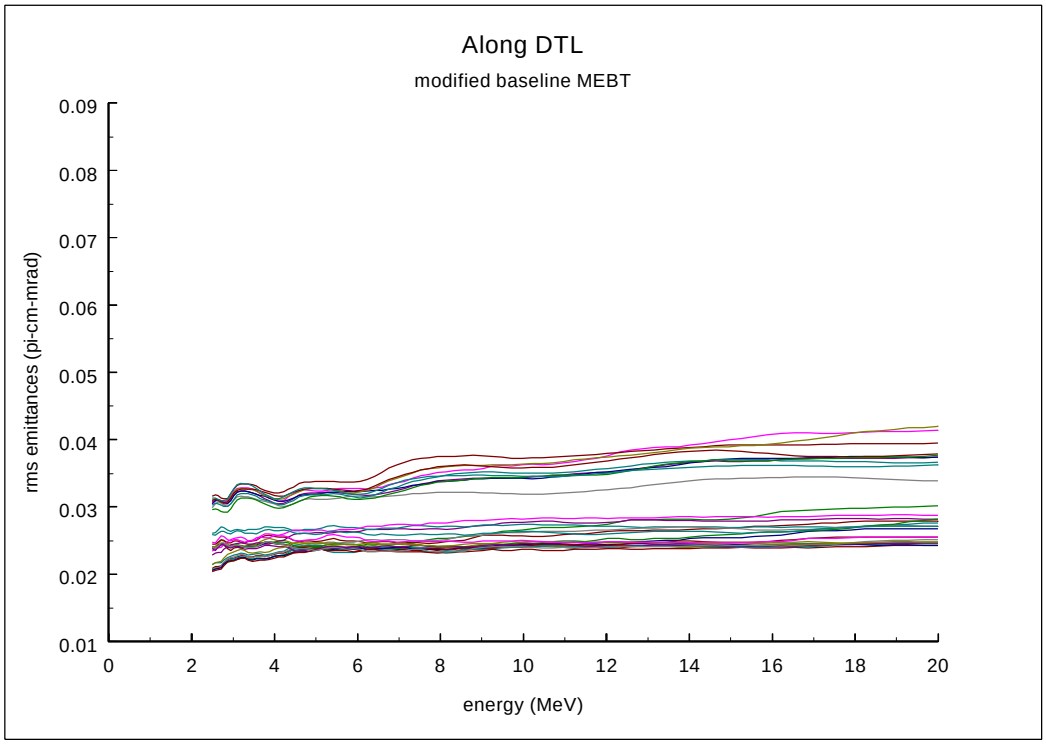

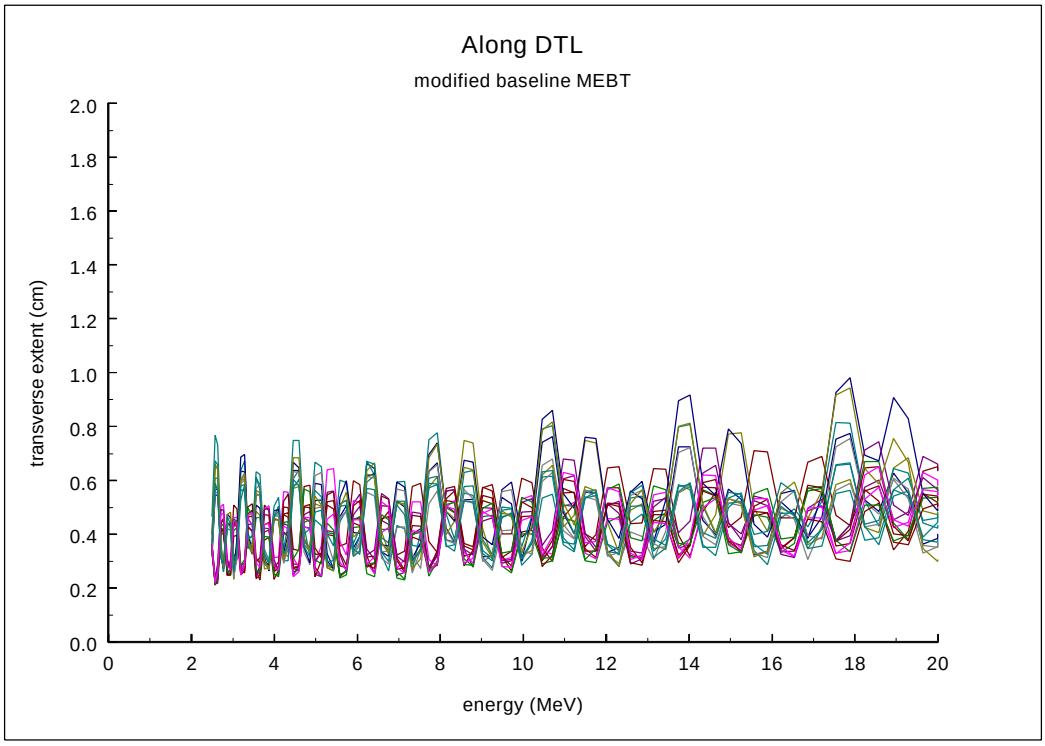

Figure 10. Transverse and longitudinal rms emittances (top) and transverse maximum beam extents (bottom) in DTL, for modified baseline MEBT.

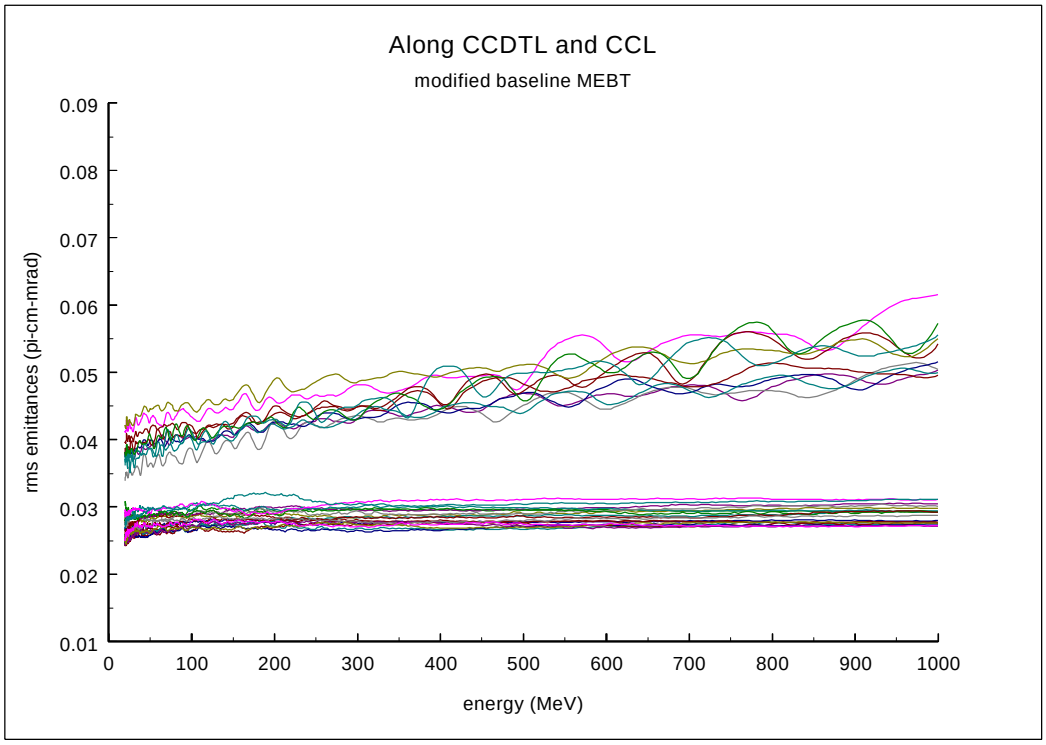

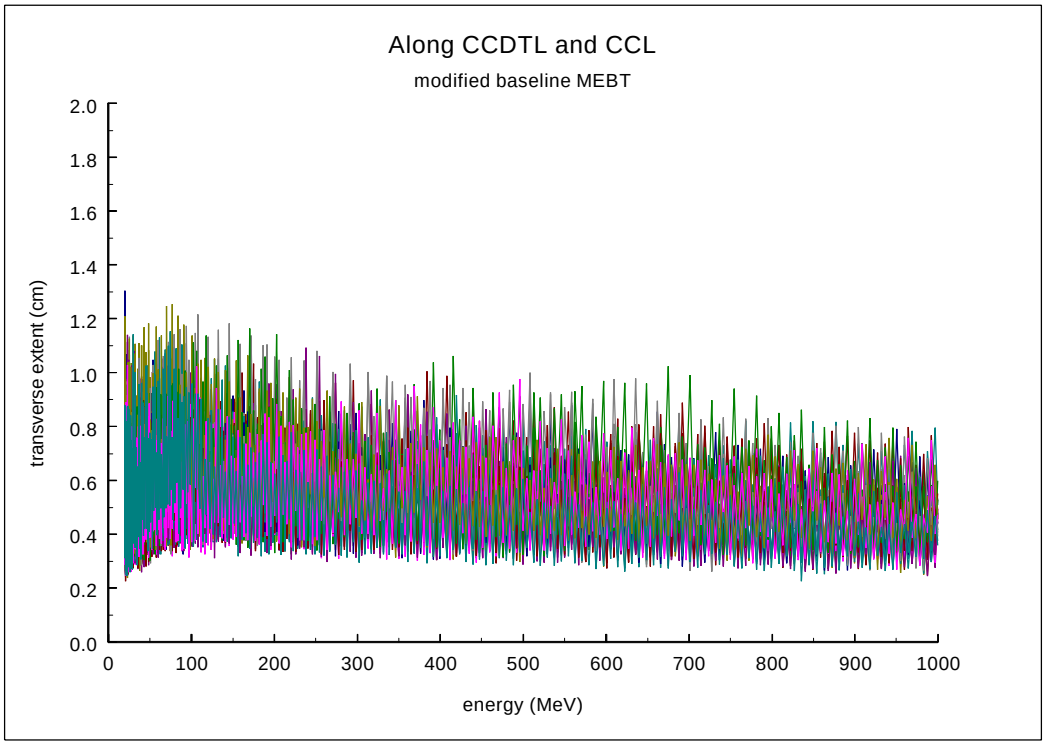

Figure 11. Transverse and longitudinal rms emittances (top) and transverse maximum beam extents (bottom) in CCDTL and CCL, for modified baseline MEBT.